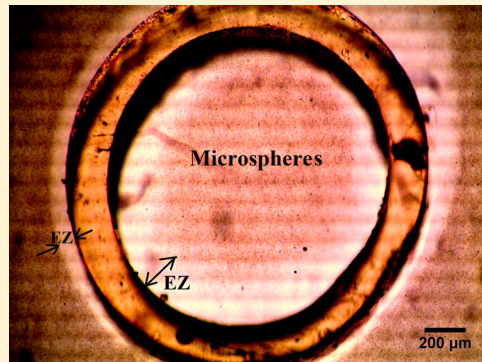


Flow through Horizontal Tubes Submerged in Water in the Absence of a Pressure Gradient: Mechanistic Considerations

Mina Rohani* and Gerald H. Pollack

Department of Bioengineering, University of Washington, Seattle, Washington 98195, United States

ABSTRACT: Self-driven flow was observed in Nafion and other hydrophilic tubes immersed in water. The intratubular flow was generated when water came in contact with the tube's hydrophilic surfaces. Flow characteristics were studied in tubes of varying size, exposed to light of different intensities and wavelengths. The results lead to the hypothesis that the flow is driven by a high concentration of protons accumulating inside the tube, creating an axial proton gradient between the inside and outside of the tube. We also demonstrate a faster flow under incident light, particularly at UV wavelengths, implying that proton generation may be driven by light.



INTRODUCTION

Fluid transport occurs in the presence of a driving force. This force may arise from a pressure gradient, an electrokinetic or magnetohydrodynamic drive, or various other phenomena.^{1,2} In any case, flow results from the conversion of any of various types of energy into kinetic energy.

Immersing Nafion in water with microspheres results in the formation of a microsphere-free zone at the interface of the hydrophilic material and water.³ Because this zone excludes various particles and solutes, it has become known as the exclusion zone or EZ. Many earlier studies have shown that the water adjacent to hydrophilic surfaces has different characteristics than bulk water, both physically and chemically.^{4,5} These hydrophilic surfaces include Nafion and various gels.³

When Nafion tubes are immersed in water, water flows continuously through the tube. Because Nafion also bears exclusion zones, we wished to test whether the flow generation was related to the EZ and furthermore what might be the flow-driving mechanism.

EXPERIMENTAL METHODS

Microsphere Suspension. Nafion tubes (Perma Pure LLC) were submerged in distilled, deionized water (Nanopure, Barnstead, 18.1 MΩ cm). To visualize the flow inside the tubes, Polybead carboxylate 1 μm microspheres (Polyscience Inc.) were suspended in the water, at a microsphere-to-water volume ratio of 1 to 300. The volume ratio was kept constant in all experiments to eliminate any effects that might arise from concentration differences.

Setup. A standard chamber was used for the experiments unless otherwise noted. The chamber was made from a rectangular polycarbonate block with a hollow cylinder cut out (8.7 mm diameter, 5.8 mm height, 350 μL volume). The bottom was covered with a glass slide, and the top was left uncovered. The Nafion tube was positioned horizontally at the bottom of the chamber and held by a thin barrier.

Figure 1 shows the chamber. Panel a shows an exploded schematic, and panel b shows the assembled chamber, ready to be filled with water.

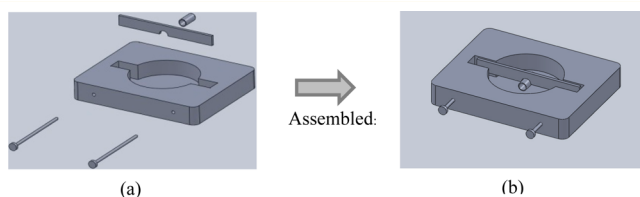


Figure 1. Experimental chamber. The chamber is 5 cm long, 2.5 cm wide, and 5.5 mm high. A glass slide is glued to the bottom. The cylindrical cavity has a diameter of 8.8 mm, a height of 5.8 mm, and a volume of 350 μL.

The thin vertical barrier, fixed with screws, has a small cut underneath to hold the tube at the bottom of the chamber. The barrier does not separate the chamber into two parts because water can flow freely above and below the barrier.

Nafion becomes hydrophilic as it is hydrated.⁶ Prior to all experiments, Nafion was allowed to prehydrate for 15 min. Each test started with a new prewashed Nafion tube. All water was taken from a Barnstead Diamond ultrapure source. The water showed some pH variation for approximately half an hour after being dispensed. In a representative test, the pH of the water, measured with a Fisher Scientific pH meter, was 5.4 immediately after leaving the Barnstead unit, 6.0 after 10 min, and 6.4 after 20 min and then formed a plateau at a pH of 6.6 by 30 min and afterward. The pH increase was found consistently and may be tied to carbon dioxide exchange. To avoid any effects of such pH variation, the water was left standing in the chamber for approximately 30 min prior to experimentation.

Figure 2 shows a cross-sectional picture of a hydrated Nafion tube immersed in a microsphere suspension. The image shows annular, microsphere-free EZs both inside and outside the tube.

Received: January 20, 2013

Revised: April 26, 2013

Published: April 30, 2013

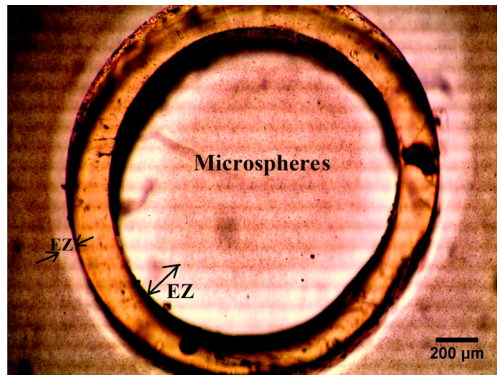


Figure 2. Cross-sectional view of a Nafion tube in an aqueous microsphere suspension. The brighter white areas show the exclusion zones from which microspheres have been expelled.

An inverted Nikon Diaphot microscope with an attached video camera (Edmund Optics) captured the flow inside the tube. The microscope's light intensity was kept constant in all experiments in order to guard against any inadvertent light effects on flow.

Flow characteristics were studied for tube lengths ranging from 1 to 5 mm and two tube diameters. The tubes' outer diameters (dry) were 840 and 1500 μm . When hydrated, Nafion tubes absorb water and expand. The final outer diameters were approximately 925 and 1800 μm , respectively. Hydrated inner diameters were 725 and 1400 μm . Tube characteristics, including both diameter and length, are summarized in Table 1.

Table 1. Tubes Categorized According to Diameters (D_1 and D_2) and Lengths (L_1 to L_5)

tube name	D (mm)	L (mm)
D1L1	0.84	1
D1L2	0.84	2
D1L3	0.84	3
D1L4	0.84	4
D2L1	1.5	1
D2L2	1.5	2
D2L3	1.5	3
D2L4	1.5	4
D2L5	1.5	5

Velocity values were measured by recording videos of microspheres flowing through the tube and using ImageJ software for particle tracking. The maximum velocity generally occurred along the tube's central axis. Throughout this Article, the values reported are those central, maximum values. An automatic program recorded the velocity every 6 min, starting 2 min after immersion in the microsphere suspension, with 2 min being the average time required for full EZ formation. EZ sizes were measured from captured images using a reference scale.

Light Source. The microscope's halogen lamp was used as the white light source. The light intensity was adjustable and measured using a power meter (Newport, model 1815C). The chamber was illuminated as uniformly as possible in order to avoid local heating. For basic experiments, the power of the white light was kept constant at 1 mW.

For the experiments using a UV source, a custom-made broadband UV-vis lamp (wavelength range 332–392 nm) was used. To study the transient impact of wavelength change on flow, a protocol was adopted to alternate between white and UV light sources, maintained at the same intensity. The sources were alternated approximately every 20 min.

Gel Preparation. In addition to Nafion tubes, we also tested poly(ethylene glycol) (PEG) channels and poly(vinyl alcohol) (PVA) tubes. To make PEG microchannels, a premade SU-8 mold was used. The mold was a simple single rectangular microchannel mold (2 mm width, 10 μm height, and 20 mm length). PEG was prepared from a low-

molecular-weight (250 g/mol) poly(ethylene glycol) diacrylate (Sigma-Aldrich) mixed with 2-hydroxy-2-methylpropiophenone (Sigma-Aldrich) to a volume ratio of 2% (98% PEG) and poured onto the mold in a Petri dish. It was then polymerized under UV light for 5 min. The polymerized PEG was transparent. The channel was left uncovered.

PVA was prepared by mixing polyvinyl alcohol with water in a ratio of 4%. For polymerization purposes, 4% borax was added. The volume ratio of the borax to PVA solution was 1 to 4. The solution was then heated for 20 min at 80 °C. The preparation required stirring until gelling was complete. Because the gel was not quite a moldable material, a conical tunnel was created by using a plastic cone as a mold (6 mm larger diameter, 2 mm smaller diameter, and 20 mm length). We surrounded the cone mold with the gel and applied some pressure to form the PVA gel. Then, the mold was removed, and the tunnel-containing gel was immersed in water for testing.

RESULTS

We consistently observed flow through the Nafion tubes as well as poly(ethylene glycol) (PEG) channels and poly(vinyl alcohol) (PVA) tunnels. The observations reported below refer mainly to the Nafion tubes. Most of the observations were made using the standard chamber (Experimental Methods). Later, we found that flow could persist for much longer in larger chambers. Those latter observations are described later in the Results.

Although a fixed microsphere concentration (volume ratio of 1 to 300) was routinely used, lower concentrations were tested, down to 10% of the standard concentration. We could find no obvious differences in flow velocities (except that fewer microspheres made detection more challenging), confirming that the presence of microspheres played no more than an incidental role in the quantification of results.

EZ Size. Before studying the flow characteristics, we measured the EZ sizes inside and outside the tube at random locations along the length. This was done before the flow started, during the course of flow, and after the flow had stopped. Some variation in inside and outside EZ sizes was observed, but we could detect no systematic changes. In one representative example, the inside EZ was measured every 10 min over 2 h. Averaging over time gave a mean EZ size of $156 \pm 20 \mu\text{m}$. The modest SD indicated that the EZ appeared to be reasonably stable over time.

Success Rate. Short tubes always resulted in flow regardless of tube diameter. For 1 and 2 mm tube lengths of both diameters, the success rate was 100% ($n = 8$).

D2L3 and D2L4 also showed a relatively high success rate of 86% ($n = 7$). When the length was increased, D2L5 showed flow about 50% of the time ($n = 6$). D2 tubes with lengths longer than 5 mm showed little or no flow.

Smaller-diameter tubes generally had lower success rates. For D1L3, the success rate was 50% ($n = 6$). D1L4 generated either very slow flow (velocity was generally lower than 2 $\mu\text{m}/\text{s}$) or no flow. Increasing the D1 length to 5 mm or longer resulted in no flow. In D1 tubes, therefore, the chance of seeing flow was high only for lengths shorter than 4 mm.

Spontaneous Flow Behavior. Velocity Variations over Time. To study the flow pattern over time, 1.5-mm-diameter, 4-mm-long Nafion tubes (D2L4) were used. The results from five tests are plotted in Figure 3. The flow generally started within the first minute. Velocity values were highest in the first 5 to 10 min and then progressively diminished over time.

Velocity as a Function of Tube Diameter and Length. Generally, we found that fluid velocities increased as the tube length increased toward an optimal value. For a D2 tube, the optimal length was 4 mm; for the D1 tube, it was 3 mm.

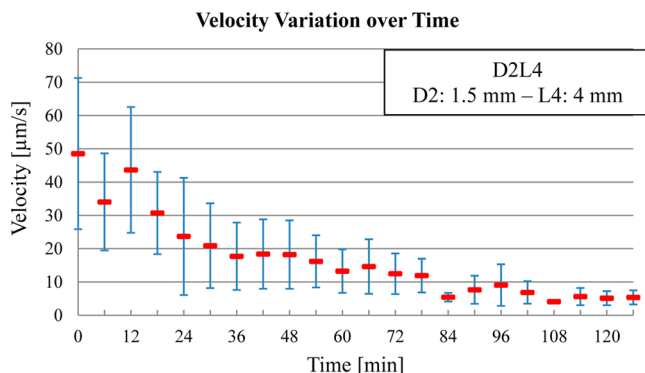


Figure 3. Flow velocity over 2 h in 4-mm-long Nafion tubes. The mean velocity ($n = 5$) is in red, and the standard deviation is in blue.

Regarding the diameter variation at constant length, experiments showed much lower velocities for smaller diameters. For example, for an L4 length, the maximum mean velocity was as large as $50 \mu\text{m/s}$ in the D2 tube, whereas in the D1 tube it did not exceed $7 \mu\text{m/s}$.

Effect of Chamber Size on Flow Velocity and Duration. Preliminary observations had shown that larger chambers produced larger and longer-lasting flows. To study these effects in detail, the total volume of fluid passing through the tube until flow stoppage was measured in differently sized chambers. D2L3 tubes were used. The smallest chamber that was routinely used (Figure 1) had a volume of $350 \mu\text{L}$, and the largest had a volume of $6000 \mu\text{L}$. Knowing the tube diameter and flow velocity, we could calculate the total volume of fluid that had passed through the tube during the entire time the flow was ongoing (Figure 4).

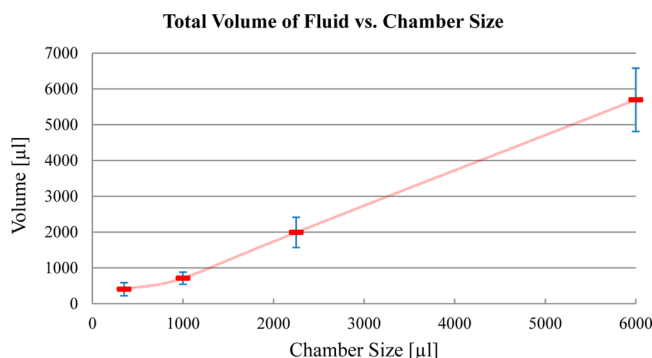


Figure 4. Volume of fluid passing through the tube (D2L3 tube) in various chamber sizes. The averaged data ($n = 3$) is in red, and the standard deviation is in blue.

The numbers shown in the plot, therefore, represent the total liquid volume transported until the flow stops. Because the stop

times differ for the respective data points, the flow durations differ as well.

We found that larger chambers resulted in larger fluid volumes. The highest volume occurred in the $6000 \mu\text{L}$ chamber, and that was also the longest-lasting, typically 1.5 days. For smaller chambers, including the standard one, the flow duration usually did not exceed 3 to 4 h. The effects of chamber size on the fluid volume were dramatic: increasing the chamber volume from 350 to $6000 \mu\text{L}$ increased the volume transported by more than 10 times, and the linearity of the curve suggested that further increases in chamber size would continue to increase the volume transported.

Flows in Gel Channels and Tunnels. We observed spontaneous flow in PEG microchannels and PVA tunnels. Furthermore, both materials showed exclusion zones qualitatively similar to those of Nafion (Figure 5). The PVA EZ was the largest, Nafion was next, and PEG was the smallest. A tapered mold was used for PVA because it was easy to remove; at the same time, the taper provided a means to check the flow direction: all of the sample cases ($n = 3$) showed flow from the larger to smaller diameter.

PVA also resulted in the highest velocity among all materials (sometimes up to $100 \mu\text{m/s}$), although the flow did not persist as long as in the Nafion tubes. PEG also led to stable flows lasting up to several hours, although the velocities (typically $5 \mu\text{m/s}$) were lower than for Nafion (typically $10 \mu\text{m/s}$).

Flow Depends on Incident Light. Effects of Light Intensity. To study the effects of light on flow, we used the microscope's lamp at a series of incident intensities. The tube size (D2L3) and chamber size ($350 \mu\text{L}$) were fixed for this and subsequent experiments on the effects of light. In each experiment, we measured the peak velocity (Figure 6). Results are shown for a representative run (a) and the average over multiple runs (b).

Effects of the Optical Wavelength. Previous studies have shown that the EZ expansion depends on the wavelength.⁷ We therefore examined the effects of different wavelengths on flow. To do this, we substituted a broadband UV source for the microscope's white light source, with optical powers set to be equal. Figure 7 shows the fluid velocity over time in the respective situations. UV gave higher velocities, but those velocities diminished more quickly than when the white light source was used.

In addition to the observations depicted in Figure 7, a special alternation protocol was used to compare the effects of the two wavelength ranges. D2L3 tubes were used in the $350 \mu\text{L}$ chamber. A protocol of 20 min alternation was followed in five experiments with similar results. Figure 8 shows a representative example.

Comparing the two colors in the plot shows that incident UV consistently induced an increase in velocity. By contrast,

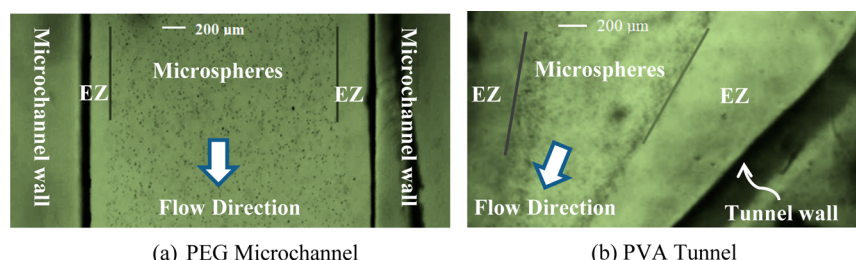


Figure 5. Exclusion zone inside (a) a PEG microchannel and (b) a PVA conical microchannel. The EZ boundary is shown by the lines.

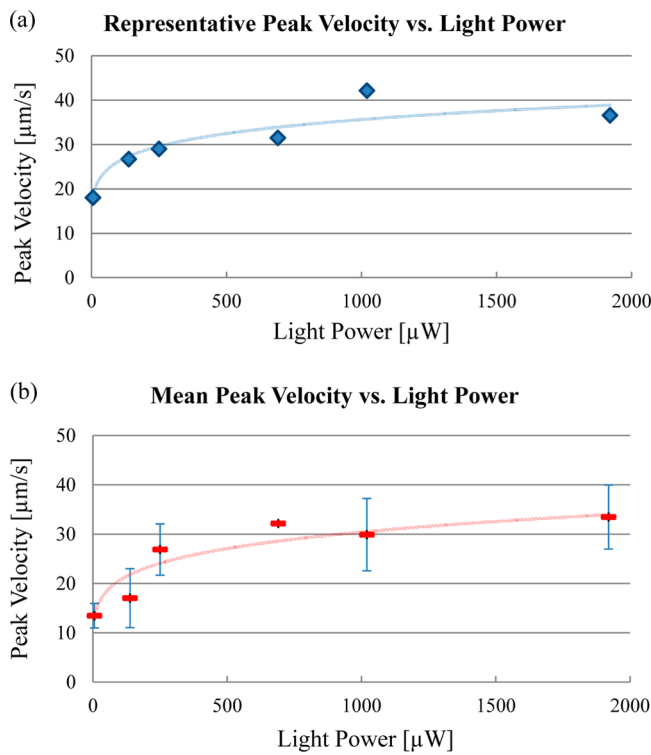


Figure 6. Effect of white light power on peak velocity: (a) representative test and (b) mean peak velocity for the respective run ($n = 4$). The means are shown in red, and the standard deviation is shown in blue. A D2L3 tube was used in a $350 \mu\text{L}$ chamber.

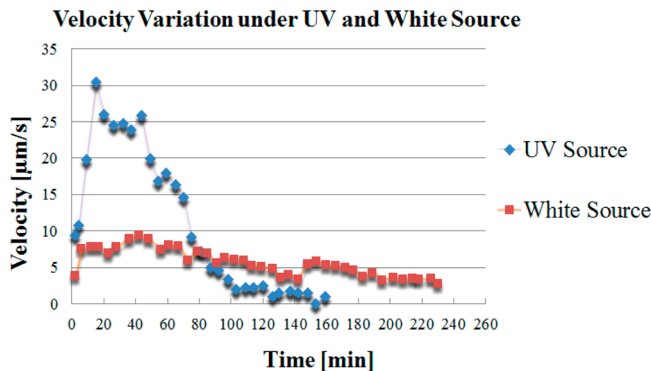


Figure 7. Velocity variation over time with the white light source and UV source at the same optical power levels. Representative runs are shown. A D2L3 tube was used in a $350 \mu\text{L}$ chamber.

replacing the UV source with the microscope's white light source generally brought about a velocity reduction relative to that of the UV source. Thus, UV wavelengths greatly enhance velocities, similar to the results shown in Figure 7.

The figure shows additional features worthy of mention. First, an overall falloff in velocity was observed over time, similar to that seen without alternation. Second, close to the 20 min mark of each period of UV illumination, the velocity began to decrease. This decrease implies that the enhancing effect of UV diminished over time, even with continued illumination.

Observing velocities under light illumination raised the question of whether heat transfer might be responsible for the increased velocity. Calculations show that the amount of energy coming from the light leads to a trivial temperature change: for the $2000 \mu\text{W}$ light intensity (the maximum used in these

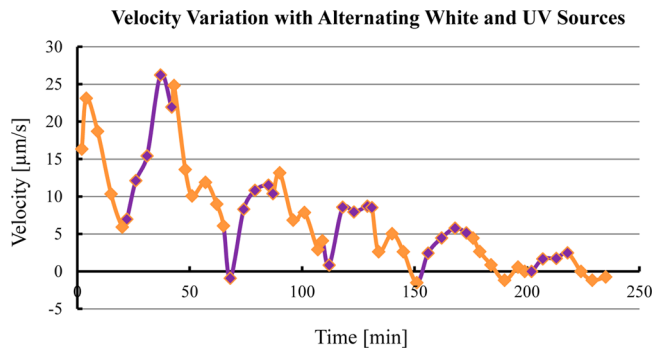


Figure 8. Effects of alternating white and UV sources on the measured velocity. Purple corresponds to the period of UV illumination, and orange corresponds to the period of white light illumination.

experiments), 0.35 mg of water in the chamber, and a specific heat of water of $1.0 \text{ cal/g } ^\circ\text{C}$, calculations show a $0.00008 \text{ } ^\circ\text{C}$ temperature rise per hour. Thus, heating effects should be inconsequential.

DISCUSSION

General Features of Flow. This Article reports the self-generation of flow inside hydrophilic tubes immersed in water. The flow phenomenon was first observed in this laboratory by Yu et al.,⁸ who showed that the flow took place not only in Nafion tubes but also in tunnels bored through poly(acrylic acid) gels. We have confirmed their result and extended the observations to include flow in PEG and PVA channels. Thus, the flows are not specific to Nafion tubes but occur in a variety of tubes and channels made from hydrophilic materials. We have also demonstrated that the energy for driving the flow comes from light.

Origin of Flow. The driving mechanism appears to come from the light-induced separation of charge. Earlier studies established a foundation for this view. When hydrophilic surfaces are immersed in water, extensive solute-free zones form.³ These exclusion zones or EZs bear charge. Generally, the EZ is negatively charged, and the water beyond the EZ is positively charged.⁹ Those studies also reported that the EZ's negative electrical potential has its maximum value close to the material surface, progressively decreasing farther from that surface. Figure 9a shows a schematic of this charge separation. Future studies should be able to measure the electrical potentials in situ and quantify the UV-based increase in charge separation.

Figure 9b illustrates how a tubular geometry creates an annular EZ, resulting in a high concentration of protons in the core of the tube. The EZ bears negative charge, and the bulk water in the core is positively charged with protons. As the proton concentration builds following the tube's immersion in water, increasing repulsion causes protons to move axially toward less positive areas outside the tube. This movement should result in a mass flow of water from inside the tube toward the outside.

The details of this process are summarized in Figure 10. As the exclusion zone builds, protons are released into the bulk water (top). The concentrations of protons will be highest near the EZ–bulk water boundary because of the protons' attraction to the EZ's negative charge. With the continued input of radiant energy and the further release of protons, the increased repulsive force among protons drives many protons toward the tube's central axis (middle). Progressively, protons occupy the core region, and the proton gradient from inside to outside exists throughout the entire tubular cross section (bottom). Those

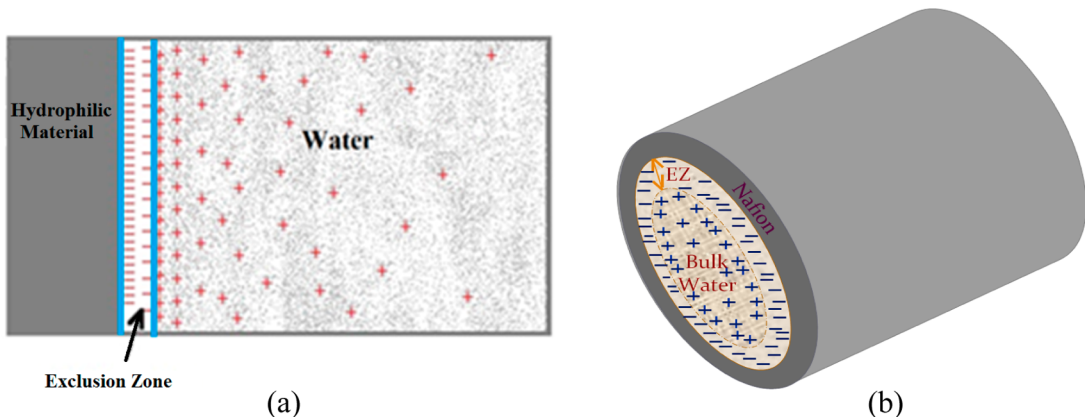


Figure 9. (a) Distribution of charge in the exclusion zone and water beyond the exclusion zone as shown by electrical potential measurements and pH-sensitive dye studies. Protons spread in bulk water, although some cling to the negatively charged EZ. (b) Disposition of charge anticipated in a tubular configuration.

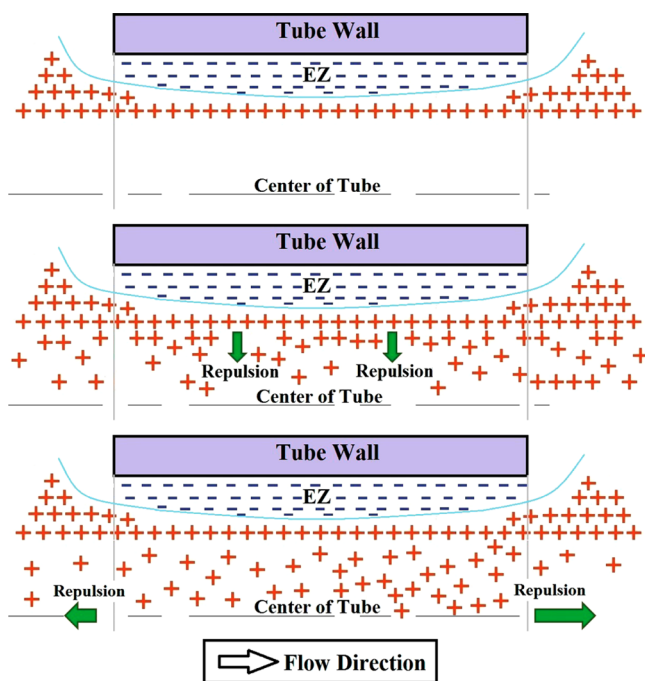


Figure 10. Protons leave the EZ, initially concentrating at the EZ boundary (top). As more charges separate, the increased numbers of protons, subject to proton–proton repulsion, begin moving toward the central axis (middle). As the concentration of protons near the central axis grows (bottom), protons begin flowing out of the tube from one end or the other (bottom).

protons near the central axis are not restrained by their attraction to the EZ and are therefore relatively free to flow axially. They drive the flow.

An expectation of this proton-based hypothesis is that protons will accumulate in the chamber. Protons leaving the interior of the tube flow into the chamber continuously. Hence, the chamber-water pH should progressively decline as flow continues. To check this expectation, we measured the pH of the chamber water before and after the flow using a standard pH probe. The pH decline was confirmed, initially at a rapid rate, which progressively decreased over time. Over 2.5 h, measurements showed a change from pH 7.48 to 2.77. When flow stopped, the pH decline stopped. Thus, the anticipated release of protons in the flow-driving process is confirmed.

Flow Direction. The flow began in a direction that was unpredictable. However, once it began, it continued in the same direction until the flow finally stopped.

The direction was probably set by some kind of asymmetry inside the tube. The proton concentration is neither perfectly uniform along the tube axis nor symmetric at the two ends, even though we tried to use uniform tubes and adjusted the incident light to be reasonably uniform over the field. Any axial asymmetry in proton concentration implies a different inside-to-outside proton gradient at the respective ends of the tube. One end's gradient eventually overcomes that of the other and directs the fluid out of the tube in the respective direction. Once that flow begins, fresh water is pulled into the rear end of the tube and gets protonated and the flow continues.

We considered several experimental approaches to try to create asymmetries purposefully. Such experiments may seem simple and trivial, but several attempts achieved only limited success. The only approach that proved successful was using tapered tubes. In that case, the flow direction was consistently toward the smaller end. Many variables can enter into the setting of direction. Serious efforts in the future may settle this interesting but challenging question.

We speculate that those instances in which flow failed to start might correspond to instances where the proton distribution remained relatively uniform along the tube. In those cases, similar proton gradients exist at the two ends; hence, one pull cancels the other. Often, in initially “unsuccessful” experiments, we perturbed the system by mixing the fluid in the chamber, presumably altering the local gradient. In most cases, flow started. Furthermore, flow began at a high success rate in the shorter tubes, where nonuniformities caused by end effects might be anticipated to dominate. This suggests that in the very long tubes in which tube effects greatly outweigh end effects some initiator might be required to prime the flow.

The question might be raised as to whether local microsphere flow genuinely represents the local flow of the liquid. To be certain, we checked this by using pH dyes, which attach to hydronium ions (protons plus water). The flow of pH dye (which turns red in the presence of protons) should therefore be representative of the flow of water. We observed that the pH dye and microspheres flowed together at the same velocity. Hence, the local microsphere flow velocity should be a valid indicator of the local water flow velocity.

Effects of Varying Parameters. Chamber Size. A key observation was that the flow lasted longer in larger chambers. In the largest chamber (6 mL), the flow duration exceeded 1.5 days, with velocities above 15 $\mu\text{m}/\text{s}$ over more than half the flow time. That value is greater than the highest velocity recorded in a standard 350 μL chamber. Decreasing the chamber size resulted in less total volume passing through the tube before flow stopped (Figure 4).

These observations fit the proton-gradient hypothesis. The hypothesis posits that the inside-to-outside proton gradient bears responsibility for driving the flow. Therefore, protons from inside the tube flow into the water outside the tube. Because larger chambers have more capacity for accepting protons without reducing the chamber pH and thereby compromising the driving gradient, those larger chambers should result in longer-lasting and more vigorous flow. That is what was found and illustrated in Figure 4.

In smaller chambers, by contrast, protons accumulate more rapidly in the chamber. Accumulation will diminish the proton gradient from inside to outside, progressively reducing the driving force and compromising the flow. That was observed as well.

Tube Diameter and Length. Larger-diameter tubes produced higher velocities. One contributing factor may be the increase in the tubular surface area, which should increase the rate of proton generation and thereby produce faster flow.

However, increasing diameter also increases the fluid volume to be moved and the load increases. Thus, the balance between increased drive and increased load needs to be considered.

This comparison is not entirely straightforward, however, because the driving force may vary over the radial dimension: the circumferential protons tend to cling to the negatively charged EZ; hence, they may not contribute much to the axial drive. The protons closer to the central axis may be more effective. Large tubes should contain more of those central axis protons. However, the exact radial distribution of those central axis driving protons is difficult to predict quantitatively, so the quantitative extent of the velocity increase with increased tube diameter is difficult to predict.

Regarding length, we found an optimum length that produced the fastest flow. For tubes longer than the optimum, the flow diminished and sometimes did not even occur. In theory, the longer tubes should generate more protons inside and hence a higher drive, and that seemed to bear out at lengths up to optimum. At the same time, the load increases proportionally with length due to a larger volume of fluid to be moved. We think the balance between these two effects controls the optimum length for the flow at each diameter.

For the latter, however, a relevant factor may be the proton concentration inside the tube. If protons are not quickly swept out of the tube, as in the shorter tubes, then their lingering presence may inhibit the further release of protons, which would diminish the flow.

Effect of Incident Light. Earlier observations on flow in Nafion tubes showed that the flow occurred spontaneously (i.e., solely by leaving the tube in the water⁸). Because the flow lasted for extended periods of time, we wondered about the source of energy for driving the flow and tested whether the driver could be light. This idea arose from previous studies, which reported that the EZ could be expanded by incident light.⁷

To carry out these studies, different light intensities were tested. At each optical power, the peak velocity was measured.

Higher light intensities resulted in larger peak velocities (Figure 6).

We also studied the effects of the energy-rich UV light in comparison to visible wavelengths. At equal power, UV produced considerably higher velocities (Figure 7). Similar results were found in experiments in which the incident light alternated between visible and UV wavelengths (Figure 8). As the presence of protons in the flowing fluid was confirmed by using pH dyes, the faster flow under UV light ought to be due to a higher rate of proton generation and charge separation. Hence, UV wavelengths may be particularly effective in separating charge and generating protons.

Changing the light intensity and/or wavelength may therefore constitute a practical means of controlling the speed of the flow. This makes Nafion (and other hydrophilic) tubes versatile fluidic pumps with no moving parts.

CONCLUSIONS

Nafion and other hydrophilic tubes were found to be self-priming fluidic pumps. The data collected in these experiments support the hypothesis that tubular flow is driven by an axial proton gradient between the inside and the outside of the tube. The effects of light intensity and wavelength support this hypothesis: higher intensities of visible light and the energy-rich UV light build larger proton gradients and thereby create faster flows. In other words, this self-driven flow is driven ultimately by optical energy.

A fuller treatment of the role of optical energy on water may be seen in a recent book.¹⁰

AUTHOR INFORMATION

Notes

The authors declare no competing financial interest.

REFERENCES

- (1) Castellanos, A. *Electrohydrodynamics*; Springer: New York, 1998.
- (2) Davidson, P. A. *An Introduction to Magnetohydrodynamics*; Cambridge University Press: New York, 2001.
- (3) Zheng, J. M.; Chin, W. C.; Khijniak, E.; Khijniak, E., Jr.; Pollack, G. H. Surfaces and interfacial water: evidence that hydrophilic surfaces have long-range impact. *Adv. Colloid Interface Sci.* **2006**, *127*, 19–27.
- (4) Szent-Gyorgyi, A. *Bioenergetics*; Academic Press: New York, 1957.
- (5) Ling, G. N. *In Search of the Physical Basis of Life*. Plenum Press: New York, 1984.
- (6) Goswami, S.; Klaus, S.; Benziger, J. Wetting and Absorption of Water Drops on Nafion Films. *Langmuir* **2008**, *24*, 8627–8633.
- (7) Chai, B.; Yoo, H.; Pollack, G. H. Effect of Radiant Energy on Near-Surface Water. *J. Phys. Chem. B* **2009**, *113*, 13953–13958.
- (8) Yu, A.; Carlson, P.; Pollack, G. H. Unexpected Axial Flow through Hydrophilic Tubes: Implications for Energetics of Water. *Eur. Phys. J. Sp. Top.* **2013**, in press.
- (9) Zheng, J. M.; Pollack, G. H. Solute Exclusion and Potential Distribution near Hydrophilic Surfaces. In *Water and the Cell*; Pollack, G. H., Cameron, I. L., Wheatley, D. N., Eds.; Springer-Verlag: Dordrecht, The Netherlands, 2006; pp 165–174.
- (10) Pollack, G. H. *The Fourth Phase of Water: Beyond Solid, Liquid, and Vapor*; Ebner and Sons: Seattle, WA, 2013.